Bull. Mater. Sci., Vol. 33, No. 3, June 2010, pp. 191–196. © Indian Academy of Sciences.

Dielectric properties of electron irradiated $PbZrO_3$ thin films

SHETTY APARNA, V M JALI*, GANESH SANJEEV[†], JAYANTA PARUI[††] and S B KRUPANIDHI[††]

Department of Physics, Gulbarga University, Gulbarga 585 106, India
[†]Microtron Centre, Mangalore University, Mangalore 574 199, India
[††]Materials Research Centre, Indian Institute of Science, Bangalore 560 012, India

MS received 26 September 2009

Abstract. **The present paper deals with the study of the effects of electron (8 MeV) irradiation on the dielectric and ferroelectric properties of $PbZrO_3$ thin films grown by sol–gel technique. The films were (0·62 μm thick) subjected to electron irradiation using Microtron accelerator (delivered dose 80, 100, 120 kGy). The films were well crystallized prior to and after electron irradiation. However, local amorphization was observed after irradiation. There is an appreciable change in the dielectric constant after irradiation with different delivered doses. The dielectric loss showed significant frequency dispersion for both unirradiated and electron irradiated films. T_c was found to shift towards higher temperature with increasing delivered dose. The effect of radiation induced increase of $\varepsilon'(T)$ is related to an internal bias field, which is caused by radiation induced charges trapped at grain boundaries. The double butterfly loop is retained even after electron irradiation to the different delivered doses. The broader hysteresis loop seems to be related to radiation induced charges causing an enhanced space charge polarization. Radiation-induced oxygen vacancies do not change the general shape of the AFE hysteresis loop but they increase P_s of the hysteresis at the electric field forced AFE to FE phase transition. We attribute the changes in the dielectric properties to the structural defects such as oxygen vacancies and radiation induced charges. The shift in T_C, increase in dielectric constant, broader hysteresis loop, and increase in P_r can be related to radiation induced charges causing space charge polarization. Double butterfly and hysteresis loops were retained indicative of AFE nature of the films.**

Keywords. **$PbZrO_3$; antiferroelectrics; irradiation effects.**

1. Introduction

Antiferroelectric type thin films have been extensively investigated for potential applications in integrated devices (Francombe 1972). They have unique dielectric properties that make them suitable for digital actuators and high charge storage capacitors (Jaffe 1961). The free energy difference between the antiferroelectric (AFE) and the ferroelectric (FE) phases makes it possible to force phase switching from the AFE to FE phase with an applied electric field (Berlincourt *et al* 1963). As a result, the associated strain changes during the forward phase switching (from AFE to FE) are suitable for the development of digital and analog micro actuator applications (Berlincourt *et al* 1964; Uchino and Nomura 1983; Gaskey *et al* 1995).

The antiferroelectric materials have unique properties such as field induced phase transition between antiferroelectric and ferroelectric phases (Shirane *et al* 1957). They are characterized by rows of dipoles with the dipole moment of adjacent rows equal but antiparallel so that in equilibrium there is no net spontaneous polarization. Thin films of the antiferroelectric compositions are interesting because of the characteristic hysteresis loop resulting from the field forced ferroelectric phase transition (Pai *et al* 1998). Lead zirconate ($PbZrO_3$) is of particular interest both as an end point of the technologically important $Pb(Zr,Ti)O_3$ (PZT) alloy system and because of the rich temperature and compositional dependent phase diagram near this end point. PZ is a room temperature antiferroelectric material (Shirane and Hoshino 1954), whose phase diagram is considerably richer below 230°C, it occurs in a complex antiferroelectric orthorhombic structure with eight formula units per cell.

To understand the radiation induced effects, we consider the production of defects by irradiation and the basic mechanisms responsible. The dielectric relaxation phenomenon is important for any thin film device, for both practical and scientific reasons. It is well known that material properties are mainly controlled by the inherent defects or charge carriers, which are produced during processing itself. The defects can also arise from the high energy electron or ion irradiation. When such devices are used in radiation environment, defects can be created in controlled way by subjecting them to irradiation by

*Author for correspondence (vmjali@rediffmail.com)

selected radiation of appropriate energy and fluence. The radiation induced charges will affect the charge distribution and thereby distort the local fields near the defects, the interface and the localized charges which will be reflected as changes in the device properties. It is of basic importance to understand the precise influence of irradiation induced charge carriers on the properties of materials in the presence of the inherent charge carriers. The devices will be under constant exposure to the ionizing radiations, so that it is desirable to study the radiation induced changes in the properties of the ferroelectric thin films.

During irradiation, high energy electron initially excites the electron–hole pair in materials via the Compton effect. Electron being a negatively charged particle, most of its energy will be dissipated by ionization effects through columbic interactions. The energy deposition of the electron increases more slowly with penetration depth due to the fact that its direction is changed so much drastically. As these hot electrons travel through the material they ionize other atoms, losing the energy of ionization while forming an electron cascade. When the electron no longer has sufficient energy to ionize additional atoms, they can be trapped at the sites of defects which do pre-exist or created by the high energy electrons themselves. In continuation with our earlier irradiation studies (Angadi *et al* 2002, 2003a–c, Jali *et al* 2004, 2007), an attempt has been made to study the effects of electron irradiation on dielectric and ferroelectric properties of PZ thin films.

2. Experimental

2.1 *Synthesis*

$PbZrO_3$ thin films were synthesized by sol–gel technique. The solutions were prepared from starting solutions of molar compositions of $Pb(CH_3COO)_2{\cdot}3H_2O$, zirconium *n*-butoxide, polyvinyl–pyrrolidone (PVP), acetyl acetone, 2-methoxyethanol and then zirconium butoxide was added to the solution followed by acetyl acetone. Deposition was done on $Pt(111)/TiO_2/SiO_2/Si$ substrate by spin coating with 3500 rpm for 30 s. Pyrolysis was done at 623 K for 5 min and annealed at 1023 K for 30 min in an oxygen environment. The thickness of the films was 0·62 μm. The details of synthesis are given elsewhere (Jayanta and Krupanidhi 2006).

2.2 *Characterization*

The crystallization behaviour was examined on both unirradiated and electron irradiated PZ thin films by X-ray powder diffraction using X-ray dffractometer (SCINTAG-3100).

2.3 *Irradiation*

Characterized thin films were subjected to irradiation at room temperature by electron beam of 8 MeV energy with delivered doses of 80, 100 and 120 kGy using Microtron accelerator facility at Microtron Centre, Mangalore University, Mangalore, India.

2.4 *Electrical measurements*

For electrical measurements, gold electrodes of around $1{\cdot}963 \times 10^{-3}$ cm^2 circular area were deposited on the top surface of the films by means of shadow masking by thermal evaporation technique with the platinum coated silicon substrate. Weak field dielectric measurements were made using impedance analyser (Keithley 3330 LCZ meter) with a drive voltage of 200 mV. The measurements were conducted in the frequency range 100 Hz–100 kHz, and temperature range, 300 K–600 K. Capacitance vs voltage measurements were conducted using impedance analyser and voltage source (Keithley 230 programmable voltage source) at 1, 10 and 100 kHz. P–E hysteresis loops were measured at 1 kHz in virtual ground mode.

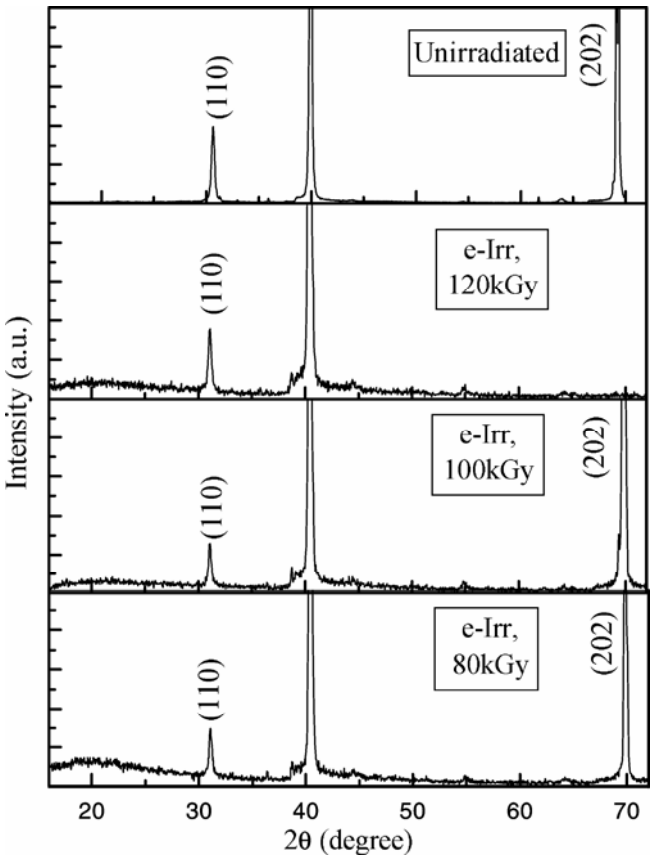

Figure 1. XRD for unirradiated and *e*-irradiated PZ thin films.

3. Results and discussion

3.1 *Structural characterization*

Figure 1 shows the XRD patterns of both unirradiated and electron irradiated (with delivered dose of 80, 100 and 120 kGy) PZ thin films. The films have the preferred (110) orientation in a pseudocubic system. The sharp peaks confirm the high crystallinity of the material. There is a decrease in the peak height intensity. Local amorphization introduced after electron irradiation is more pronounced on lower 2θ side.

3.2 *Dielectric properties*

3.2a *Dielectric constant and loss*: The variation of room temperature dielectric constant with frequency for unirradiated and electron irradiated (with delivered dose of 80, 100 and 120 kGy) PZ thin films are as shown in figure 2. There is no appreciable decrease in the dielectric constant with frequency for unirradiated films. But, there is an appreciable change after irradiation with different delivered doses. The room temperature dielectric constant of unirradiated PZ thin films at 10 kHz is 108·11. This is observed to increase with increase in delivered dose. The variation of room temperature dielectric loss ($\tan\delta$) for both unirradiated and electron irradiated PZ films are shown in figure 3. The dielectric loss showed significant frequency dispersion for both unirradiated and electron irradiated films.

3.2b *Dielectric phase transition*: The samples were heated above 573 K and dielectric response with temperature was recorded in heating cycle itself. Figure 4 shows the temperature response of the dielectric constant $\varepsilon'(T)$ of unirradiated and electron irradiated films. At different measured frequencies, for unirradiated films, the dielectric phase transition (T_c) between antiferroelectric phase and paraelectric phase is 498 K (Jayanta and Krupanidhi 2006). But, T_c was found to shift towards higher temperature with increasing delivered dose. For 120 kGy delivered dose, the T_c is 513 K. The shift of T_c could be related to strain near the contact electrodes. Similar results were reported by Bittner *et al* (2004) for the same sample under neutron irradiation. The effect of radiation induced increase of $\varepsilon'(T)$ is related to an internal bias field, which is caused by radiation induced charges trapped at grain boundaries. It is well known that internal bias field increases $\varepsilon'(T)$ near T_c in PZ (Shirane *et al* 1951).

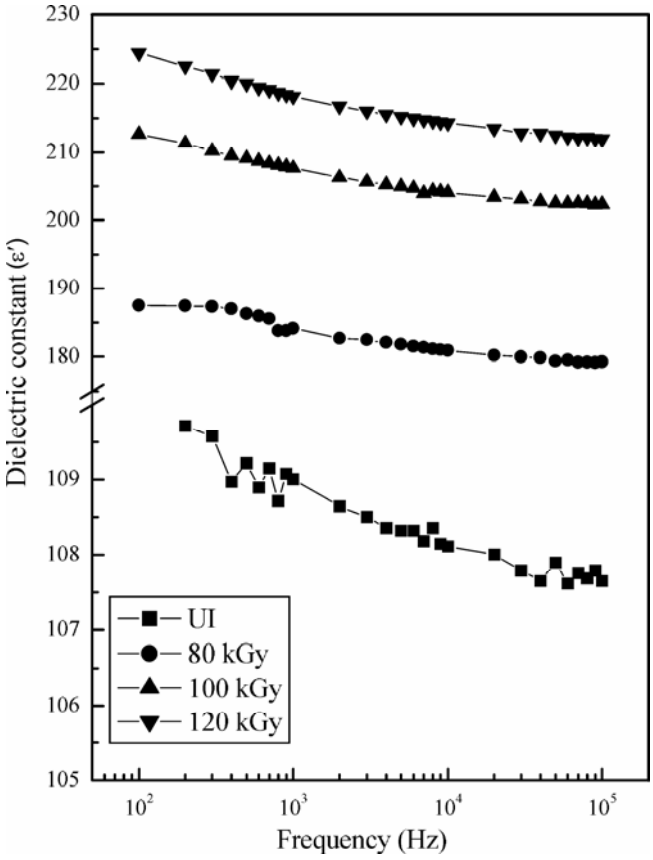

Figure 2. Variation of *RT* ε' with frequency for unirradiated and *e*-irradiated PZ thin films.

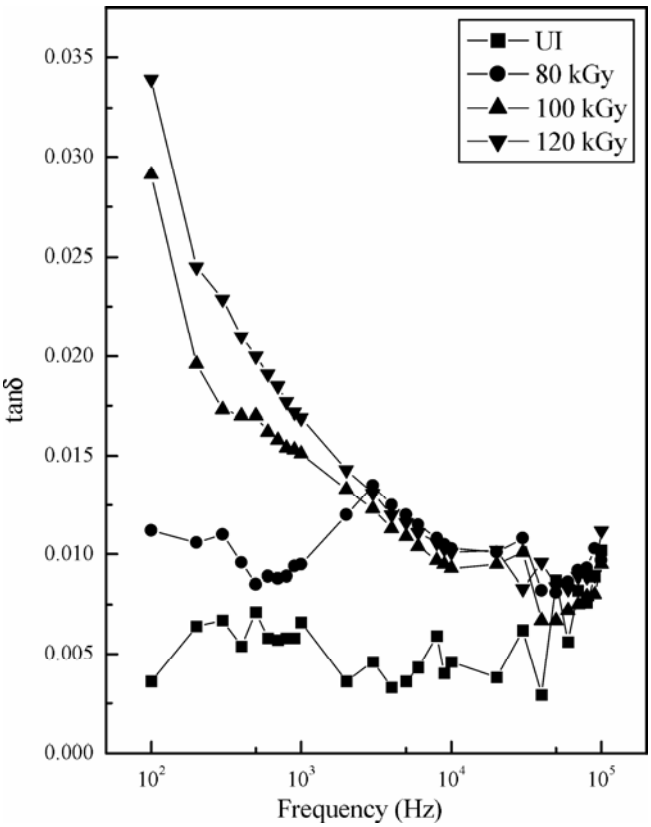

Figure 3. Variation of *RT* $\tan(\delta)$ with frequency for unirradiated and *e*-irradiated PZ thin films.

The irradiation of PZ films causes an increase in the dielectric constant that can be explained by radiation induced internal charges. An increase of charges leads to an increase of ε' at a certain grain size (Shih *et al* 1994). Also, a radiation induced internal bias field forces the surrounding area to change from AFE to FE state. But, it is observed that for 100 kGy and 120 kGy the ε'_{max} is less than the dielectric maxima at 80 kGy. The ε'_{max} values measured at 10 kHz, at T_c for all the films are shown in table 1. It is observed that the ε'_{max} increases by about 53% for the films with delivered dose, 80 kGy. It is observed that with further increase in the delivered dose above 80 kGy, the ε'_{max} dropped by 46% for 120 kGy. The decrease in the dielectric constant may be due to the pinning of the domains by the radiation induced defects which decreases the total polarization and hence dielectric constant. The variation of the dielectric loss (tan δ) with temperature for unirradiated and electron irradiated (delivered doses of 80, 100 and 120 kGy) films are shown in figure 5. Tan δ at T_c is more compared to room temperature value both in unirradiated and electron irradiated films. The tan δ and T_c for unirradiated and electron irradiated films with a delivered dose of 120 kGy are 0·0139 and 0·0317, respectively. It implies that tan δ increased after irradiation.

3.3 *Capacitance–voltage measurements*

The variation of the capacitance with voltage was done in the sequence of negative–positive–negative bias direction with a d.c. bias step of 0·2 V on both unirradiated and electron irradiated PZ thin films. The room temperature variation of capacitance with voltage for unirradiated and electron irradiated films are shown in figure 6. The presence of characteristic double butterfly loop confirms the antiferroelectric nature of PZ thin films, though there were minor deviations in the forward and backward switching fields.

The double butterfly loop is retained even after electron irradiation to the different delivered doses. It is observed from figure 6 that the dielectric constant (peak height) increased with increase in the delivered dose. The asymmetry remained after irradiation to different delivered doses. The switching voltages with corresponding C_{max} values for unirradiated and electron irradiated films are tabulated in table 1.

The C–V behaviour in the PZ films can be explained in the following way. The dielectric constant increases with d.c. bias in AFE–FE transition. The individual antiferroelectric micro regions in the presence of d.c. bias would

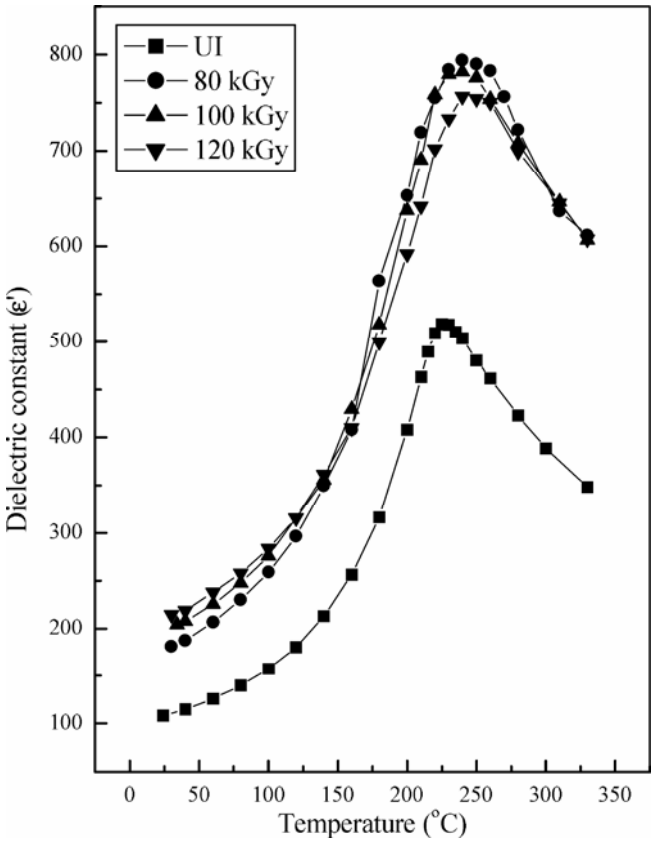

Figure 4. Variation of ε' with temperature for unirradiated and *e*-irradiated PZ thin films.

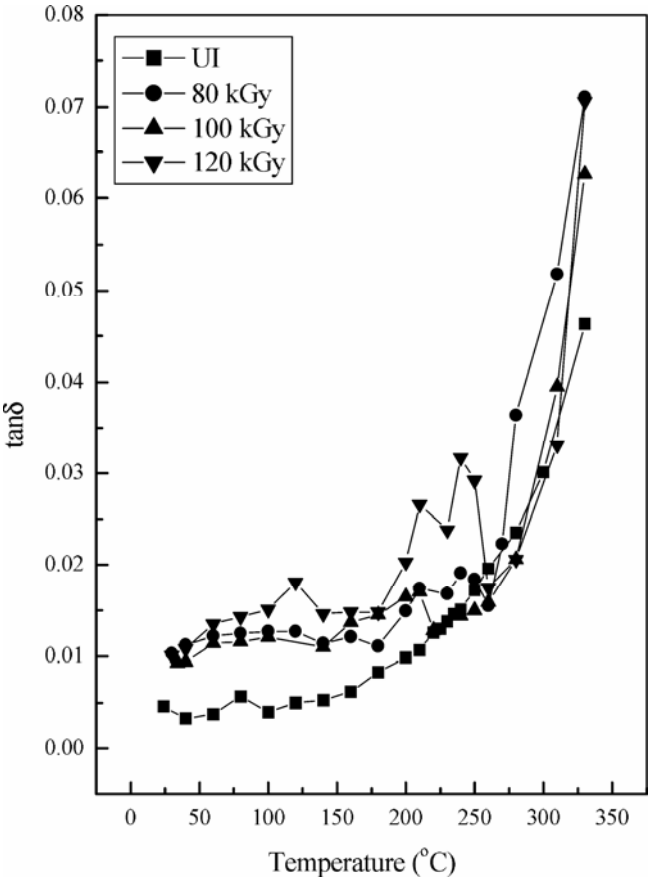

Figure 5. Variation of tan δ with temperature for unirradiated and *e*-irradiated PZ thin films.

Table 1. Summary of results of electron irradiation (with different delivered doses) effects on the various properties of PZ thin films.

	$PbZrO_3$			
		e-irradiated (kGy)		
Property	Unirradiated	80	100	120
ε', 27°C, 10 kHz	108·11	180·89	204·02	214·33
tan δ, 27°C, 10 kHz	0·0046	0·0103	0·0093	0·0101
T_c (°C)	225	240	240	240
ε'_{max}, at T_c, 10 kHz	518·22	794·24	782·11	756·78
$+V_c$ (V), 27°C, 100 kHz	12·9	11·8	12·9	11·8
$-V_c$ (V), 27°C, 100 kHz	–11·4	–11·3	–12·4	–13·5
$+C_{max}$, 27°C, 100 kHz, (pF)	674·6	809·1	970·3	941·2
$-C_{max}$, 27°C, 100 kHz, (pF)	674·6	797·8	929·9	936·6
P_s, 27°C, 1 kHz ($\mu C/cm^2$)	19	30·91	35·16	36·27
P_r, 27°C, 1 kHz ($\mu C/cm^2$)	0·82	1·97	1·99	2·36
$+E_C$, 27°C, 1 kHz (kV/cm)	25·6	59	53·86	56

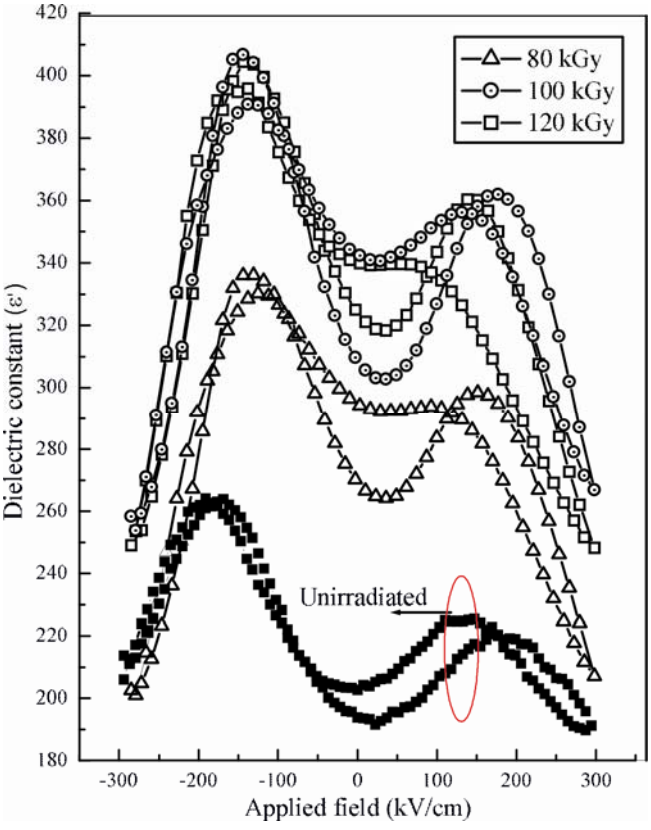

Figure 6. Variation of *RT* ε' with applied field for unirradiated and *e*-irradiated PZ thin films.

become ferroelectric. As the ferroelectrics have higher dielectric constant than antiferroelectric materials, up to the field level corresponding to the antiferroelectric–ferroelectric phase transition, the dielectric constant will continue to increase. Once the system reaches a ferroelectric phase, the capacitance of the system decreases. This is because the dielectric constant is negative derivative of the polarization with respect to applied field, during enhancing the polarization and saturation of polarization processes of ferroelectric state, the capacitance of the system decreases.

3.4 *Hysteresis measurements*

The room temperature *P–E* curves for unirradiated and electron irradiated PZ thin films at 35 V are shown in figure 7. The presence of a typical double hysteresis loop in the polarization vs electric field at room temperature establishes the antiferroelectric nature. This is observed for both unirradiated and electron irradiated films. The value of saturation polarization (P_s) is 19 $\mu C/cm^2$ at an applied electric field of 514·7 kV/cm for unirradiated films and is found to increase with increasing delivered dose. At 120 kGy delivered dose, the P_s is 36 $\mu C/cm^2$ at the same measured field. The unirradiated films exhibited a slim loop. As the field is increased and with increase in the delivered dose, the stress is removed and the area under the loop increases. The broader hysteresis loop seems to be related to radiation induced charges causing an enhanced space charge polarization. It is also observed that the P_r increased after electron irradiation. This increase in P_r could be attributed to radiation induced charges (space charge polarization) and may be a small contribution from the uncompensated shift of the Pb atoms in *c*-direction (Dai *et al* 1995; Teslic and Egami 1998) caused by oxygen vacancies. Further, an internal bias field, caused by charges trapped at grain boundaries, could force some parts of the AFE film into the FE state, this also increases P_r.

The double hysteresis loop is retained even after electron irradiation. Radiation-induced oxygen vacancies do not change the general shape of the hysteresis loop, but they increase P_s value at the electric field forced antiferroelectric to ferroelectric phase transition (Bittner *et al* 2004). These vacancies recombine partly with oxygen

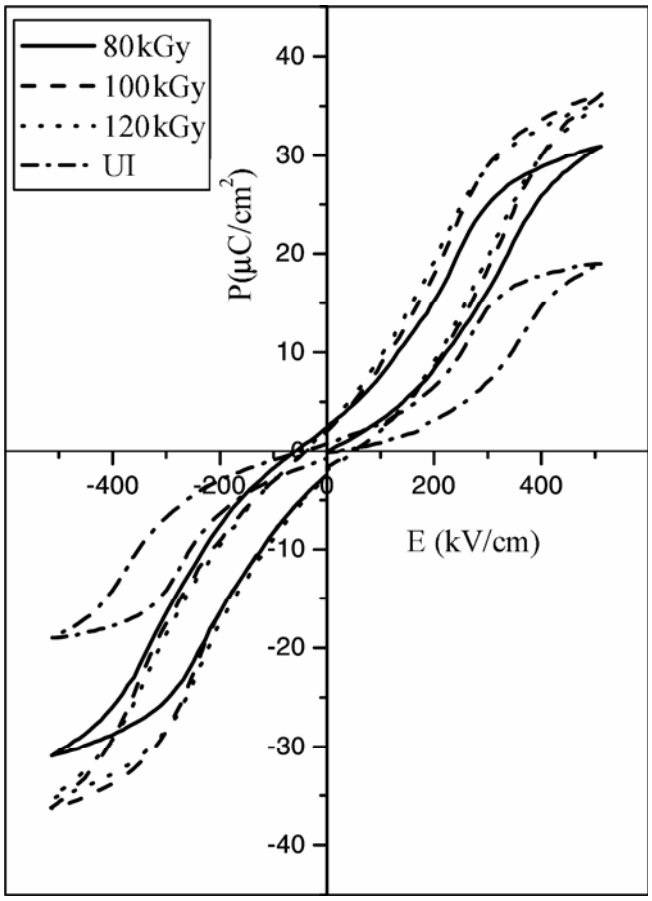

Figure 7. *RT P–E* curve for unirradiated and *e*-irradiated PZ thin films at 35 V.

interstitials during heat treatment. Further, the influence of oxygen vacancies could also be reduced by trapping mobile charge carriers which would also tend to restore the initial hysteresis loop. In addition, the interfaces are also affected by oxygen vacancies, which seem to accumulate preferably at the film/electrode interface and damage the interfacial mechanical boundary. The variation of P_s ($\mu C/cm^2$) with delivered dose is tabulated in table 1.

4. Conclusions

The required films were synthesized by sol–gel technique. After electron irradiation the induced local amorphization was reflected in the XRD. We attribute the changes in the dielectric properties to the structural defects such as oxygen vacancies and radiation induced charges. The shift in T_C, increase in dielectric constant, broader hysteresis loop, and increase in P_r can be related to radiation induced charges causing space charge polarization. Double butterfly and hysteresis loops were retained indicative of AFE nature of the films. Due to removal of residual stress there may be an observed saturation in the polarization hysteresis. The films were sensitive to electron irradiation instead of being radiation hard.

Acknowledgement

This work was carried out under the Project No. 2004/34/18-BRNS supported by the Board of Research in Nuclear Science, Department of Atomic Energy, Bhabha Atomic Research Centre, Mumbai.

References

Angadi B, Jali V M, Lagare M T, Kini N S, Umarji A M, Ravi Kumar, Arora S K and Kanjilal D 2002 *Nucl. Instrum. & Meth. Phys. Res.* **B187** 87

Angadi B, Jali V M, Lagare M T, Bhat V V, Umarji A M and Ravi Kumar 2003a *Rad. Meas.* **36** 635

Angadi B, Victor P, Jali V M, Lagare M T, Ravi Kumar and Krupanidhi S B 2003b *Mater. Sci. Eng.* **B100** 93

Angadi B, Victor P, Jali V M, Lagare M T, Ravi Kumar and Krupanidhi S B 2003c *Thin Solid Films* **434** 40

Berlincourt D, Jaffe H, Krueger H H A and Jaffe B 1963 *Appl. Phys. Letts* **3** 90

Berlincourt D, Krueger H H A and Jaffe B 1964 *J. Phys. Chem. Solids* **25** 659

Bittner R, Humer K, Wever H W, Kundzins K, Sternberg A, Lesnyh D A, Kulikov D V and Trushin Y V 2004 *J. Appl. Phys.* **96** 3239

Dai K, Li J F and Viehland D 1995 *Phys. Rev.* **B51** 2651

Francombe M H 1972 *Thin Solid Films* **13** 413

Gaskey C J, Udayakumar K R, Chen H D and Cross L E 1995 *J. Mater. Res.* **10** 2764

Jaffe B 1961 *Proc. IRE* **49** 1264

Jali V M, Aparna S, Apurba Laha, Ganesh and Krupanidhi S B 2004 *NSFD-XIII Proceedings* (University of Delhi)

Jali V M, Aparna S, Ganesh Sanjeev and Krupanidhi S B 2007 *Nucl. Instrum. & Meth. Phys. Res.* **B257** 505

Jayanta Parui and Krupanidhi S B 2006 *J. Appl. Phys.* **100** 044102

Pai N G, Xu B and Cross L E 1998 *Integr. Ferroelectr.* **22** 501

Shirane G and Hoshino S 1954 *Acta Crystallogr.* **71** 203

Shirane G, Swaguchi E and Takagi Y 1951 *Phys. Rev.* **84** 476

Shirane G, Swaguchi E and Takagi Y 1957 *Phys. Rev.* **105** 849

Shih W V, Shih W H and Aksay I A 1994 *Phys. Rev.* **B50** 15575

Teslic S and Egami T 1998 *Acta Crystallogr. Struct. Sci.* **B854** 750

Uchino K and Nomura S 1983 *Ferroelectrics* **50** 1913